General Disclaimer

One or more of the Following Statements may affect this Document

- This document has been reproduced from the best copy furnished by the organizational source. It is being released in the interest of making available as much information as possible.

- This document may contain data, which exceeds the sheet parameters. It was furnished in this condition by the organizational source and is the best copy available.

- This document may contain tone-on-tone or color graphs, charts and/or pictures, which have been reproduced in black and white.

- This document is paginated as submitted by the original source.

- Portions of this document are not fully legible due to the historical nature of some of the material. However, it is the best reproduction available from the original submission.

OPERATING SAFETY OF DIELECTROPHORETIC PROPELLANT MANAGEMENT SYSTEMS

Final Report

Covering the Period
April 24, 1967 to March 31, 1968

Dynatech Report No. 768

by:

John R. Blutt
Advanced Systems Department

Contract No. NAS 8-20553
Control No. 1-7-52-20110

Prepared for:

National Aeronautics and Space Administration
George C. Marshall Space Flight Center
Huntsville, Alabama 35812

March 31, 1968

OPERATING SAFETY OF DIELECTROPHORETIC PROPELLANT MANAGEMENT SYSTEMS

Final Report

Covering the Period
April 24, 1967 to March 31, 1968

Dynatech Report No. NONE

by:

John R. Blutt
Advanced Systems Department

Contract No. NAS 8-20553
Control No. 1-7-52-20110

Prepared for:

National Aeronautics and Space Administration
George C. Marshall Space Flight Center
Huntsville, Alabama 35812

March 31, 1968

DYNATECH CORPORATION
17 Tudor Street
Cambridge, Massachusetts 02139

FOREWORD

This report covers the third phase of a program conducted by Dynatech Corporation, Cambridge, Massachusetts, under the NASA Contract NAS 8-20553 entitled "Research and Design of a Practical and Economical Dielectrophoretic System for the Control of Liquid Fuels under Low Gravity Environmental Conditions." Phase I of this program was to design a dielectrophoretic baffle for the control of the fundamental slosh mode in propellant tanks under low gravity conditions. Phase II was a parametric design and optimization study of a dielectrophoretic liquid control system. Phases I and II have been presented under separate reports. Phase III, the subject of this report, is entitled "Identification and Elimination of All Known Hazards with Hydrogen and Oxygen Propellants and Helium Pressurant in Electric Fields with Typical Dielectrophoretic Electrode, Support, and Feedthrough Designs," and was initiated under the NASA PR No. 1-7-52-20110.

A part of the work on electrical breakdown and materials compatibility with oxygen was performed in conjunction with a second program, Air Force Contract No. AF 33(615)-3583, entitled "Research for the Design of Experimental Liquid Oxygen Converters."

Mr. John R. Blutt was the principal investigator* for Dynatech Corporation on Phase III of this program. The full-scale tests were performed under sub-contract by the Lockheed Missiles and Space Company, Sunnyvale, California, where Mr. H. L. Jensen was project manager and Mr. Larry Mellema was the test engineer. The work was monitored by the Propulsion and Vehicle Engineering Laboratory, Marshall Space Flight Center, Huntsville, Alabama. Mr. Herman Beduerftig was Project Engineer for NASA.

This report covers work performed from April 24, 1967 through March 31, 1968.

---

*Program initiated with Dr. E. J. Fahimian as principal investigator.

ABSTRACT

An experimental program was conducted with small-scale and full-scale dielectrophoretic electrodes to demonstrate the safety of a typical dielectrophoretic propellant orientation system with oxygen and hydrogen propellants and helium pressurization. It was shown that small-scale electrical breakdown tests can be used to predict the performance of a full-scale system. Aluminum and stainless steel electrodes and Teflon electrode supports were demonstrated to be compatible with both oxygen and hydrogen even in the presence of intense electrical discharges having energy levels far exceeding those anticipated in any practical system. Electrical breakdown guidelines were established for the design of safe dielectrophoretic orientation systems.

TABLE OF CONTENTS

TABLE OF FIGURES

LIST OF TABLES

Section 1
INTRODUCTION AND SUMMARY

Analytical and parametric design studies* have shown that dielectrophoretic liquid expulsion devices for orbital tankers are significantly lighter than such competitive techniques as settling rockets, surface tension devices, and expulsion bladders. The primary objective of this program was to experimentally obtain practical engineering data to enable the identification and elimination of all potential safety hazards associated with the use of these dielectrophoretic systems for the control of cryogenic liquid oxygen and liquid hydrogen with gaseous helium pressurization. The emphasis throughout the program was on the collection of directly useful engineering data with actual electrode designs.

The program was conducted in three steps: 1) determination of the compatibility of the electrode and insulating support materials with oxygen and hydrogen environments, 2) generation of baseline data on electrical breakdown in oxygen/helium and hydrogen/helium mixtures using small-scale model electrode elements, and 3) verification of the extrapolation of small-scale electrical breakdown data to an actual system by a series of "full-scale" tests.

The materials compatibility tests were performed by subjecting small samples of the test materials to electrical arcs in atmospheres of oxygen or hydrogen over a wide range of temperature and pressure. Electrical discharges with total energy dissipation several orders of magnitude greater than would be encountered in any practical dielectrophoretic liquid expulsion system were shown to be incapable of initiating explosions or flames with either aluminum or stainless steel electrodes or with Teflon insulating supports in oxygen or hydrogen atmospheres at pressures from 15 psia to 100 psia and temperatures from 200° K to 77° K.

The data from electrical breakdown tests using small-scale electrode elements, was correlated on the basis of the Paschen similitude function (Pd/T). This data was in good agreement with data later obtained with "full-scale" tests (6" wide electrodes

*Conducted under Phase II of this contract, NAS 8-20553 and under NAS 10-4606.

with 1" and 3" spacing in a 41.5" diameter spherical tank). By introduction of a suitable factor of safety in a practical electrode design (safety factor defined as breakdown voltage divided by design operating voltage) the small-scale tests can be used with confidence to establish the voltage limit.

Section 2
MATERIALS COMPATIBILITY

The materials required for the fabrication of a dielectrophoretic propellant management system are a metal for the electrodes and feedthrough conductor and a non-metal insulator for the electrode supports and feedthrough insulation. These materials must be compatible with the cryogenic oxygen or hydrogen environments under pressures up to 75 - 100 psia in the presence of electrical discharges with total energy dissipation on the order of 7.5 joules. Even though electrical breakdown will not occur in a properly designed system under normal operating conditions, the system design must be safe under all adverse situations.

The Defense Metals Information Center has established materials compatibility classifications for corrosion resistance, shock sensitivity, and tendency to decompose the propellant. As a rule, the Center classifies copper, brass, aluminum and some of its alloys, monel, nickel, and the austenitic or 300 series stainless steels as satisfactory for use at cryogenic temperatures. The ferritic and martensitic stainless steels and carbon steels are not recommended because of their poor ductility at low temperatures.

The metals specifically listed as generally compatible with liquid hydrogen are:

300 series stainless steels
Type 410 stainless steel
1100 aluminum
5052 aluminum
4043 aluminum
2024-T aluminum
1100-T aluminum
Haynes 21
Molybdenum
Nickel
Monel
Inconel
High nickel steels
Titanium

Those generally compatible with liquid oxygen are:

300 series stainless steel
Aluminum
Copper
Bronze
Brass
Monel
Everdur
Nickel
Silver Solder
Inconel

The use of organic materials is limited because of the effect of the cryogenic temperature on their physical properties. The non-metals generally compatible with liquid hydrogen are:

Teflon
Nitryl rubber
Silicone rubber
Bakelite
Micarta
Lucite
Graphite

Those accepted for use with liquid oxygen are:

Teflon
Kel-F
Asbestos
Special silicone rubbers
Viton
Fluorel

After consideration of the special requirements of the dielectrophoretic system design, two metals, 304 stainless steel and aluminum, and one non-metal, Teflon, were selected for further compatibility testing in oxygen and in hydrogen in the presence of electrical discharges.

2.1 Materials Compatibility Test Apparatus

A special test apparatus (Fig. 1) was constructed to conduct tests to determine materials compatibility with oxygen and hydrogen in the presence of electrical breakdown. A pressure vessel was constructed to permit the testing of small samples under the following conditions:

a. Pressure -- 15 psia to 100 psia
b. Temperature -- ambient to liquid nitrogen temperature
c. Breakdown voltage -- to 120 KV dc
d. Breakdown energy -- to 7.5 joules

The test vessel was mounted in a steel test booth for safety.

2.2 Metals Compatibility Tests

Tests were conducted to demonstrate the compatibility of 304 stainless steel and aluminum with oxygen and hydrogen in the presence of electrical breakdown. Three types of test samples were used: 3/4" diameter spheres, thin sheets representative of an actual electrode, and .020" diameter wires.

The first series of tests was conducted in gaseous hydrogen and oxygen and in liquid oxygen, all at atmospheric pressure. The objective was to determine whether an explosion or fire could be initiated in the metal by the discharge of electrical energy in single arcs of up to 7.5 joules.

The second series of tests was essentially a repeat of the first series but with pressure added as a variable. Pressures ranging from 15 psia to 100 psia were tested.

In all of these tests (80 to 100 discharges in all) there was not a single incidence of a fire or explosion. Even when a continuous arc from a .020" diameter aluminum wire in pure gaseous oxygen caused the wire to glow red there was no fire. In fact, there was no indication of pitting or any other hint of a reaction from the electrical arcs.

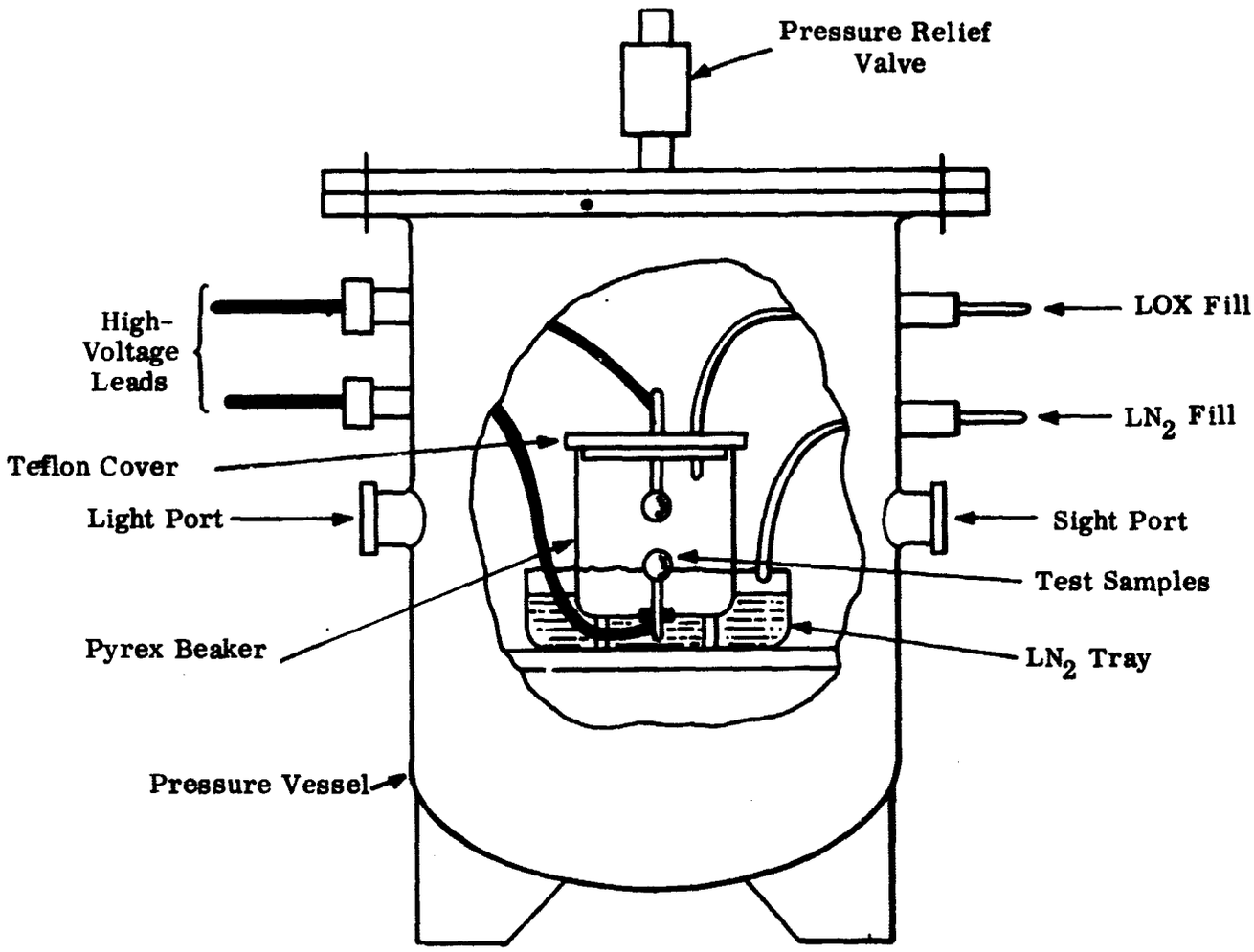

Fig. 1. Compatibility Test Apparatus

In addition to the tests run specifically to examine materials compatibility with small material samples, all of the subsequent electrical breakdown tests, with thousands of arcs under the full range of thermodynamic conditions, were completed without a single incidence of fire or explosion.

The conclusion of these tests is that the electrical energy stored in any typical dielectrophoretic electrode array is not sufficient to initiate any form of dangerous reaction between the electrode materials and the stored propellants.

2.3 Teflon Compatibility Tests

The most severe test of the compatibility of Teflon, an electrical insulator, with oxygen or hydrogen in the presence of an electrical breakdown, is an arc along the surface of the Teflon.

A sequence of tests similar to those in Section 2.2 was conducted to test the compatilibity of Teflon; that is, first a series of tests in oxygen and in hydrogen at atmospheric pressure and then a series of tests at increased pressures.

In all single spark tests at energies as high as 7.5 joules there was no evidence of a reaction with the Teflon. Only by maintaining a continucus arc, a condition that would never be realized in an actual application, could any evidence of damage be seen. In this case all that happened was that a track was formed in the Teflon where the arc decomposed the material. No fire resulted. The track formed was perfectly clean with no sign of carbon or other product that could constitute a permanent short circuit. All the products of decomposition are gaseous.

One further test was conducted to examine the burning characteristics of Teflon with liquid oxygen. To initiate burning the Teflon sample was dipped in kerosene before installation into the test vessel. The arc ignited the kerosene immediately. The kerosene burned fiercely in the pure oxygen atmosphere, decomposing part of the Teflon in the process. Once the kerosene had been consumed, however, the fire extinguished itself. The heat of combustion of the Teflon is not sufficient to raise the temperature of the remaining material from liquid oxygen temperature to the reaction temperature. The flame was not self sustaining.

Section 3
ELECTRICAL BREAKDOWN

Tests were conducted to determine the electrical breakdown characteristics of oxygen and hydrogen with various concentrations of helium. The effects of pressure and temperature were measured. Initial tests using parallel disc electrodes and small-scale elements of an actual electrode were used to establish baseline electrical breakdown data. Later tests using a full-scale electrode in a 41.5-inch diameter tank (see Section 4) were conducted to demonstrate that the breakdown data derived from the small-scale tests could be extrapolated with confidence for the engineering design of an actual dielectrophoretic system.

3.1 Small-Scale Test Apparatus

A special cryogenic pressure test apparatus (Fig. 2) was used to conduct the electrical breakdown tests. The test chamber was a 16" diameter, 30" high cylindrical pressure vessel with three 2" viewing ports. The chamber was wrapped with a LN_2 cooling line. The chamber was fabricated from 304 stainless steel to permit testing from atmospheric pressure to 100 psig at liquid nitrogen temperature.

A typical test sequence would proceed as follows:

1. Install test module
2. Pressurize to 90 psig with N_2 gas to check for leaks (leak rate < 1 psi/min).
3. Release pressure to atmospheric.
4. Evacuate.
5. Backfill and pressurize with test gas to approximately 85 psig.
6. Perform series of tests, slowly increasing the voltage until breakdown occurs. Eight to ten breakdowns are made at each pressure. The highest pressure tests are run first and the pressure then reduced by venting and breakdown tests continued at each pressure down to atmospheric pressure.
7. Vent to atmospheric.
8. Purge with nitrogen.

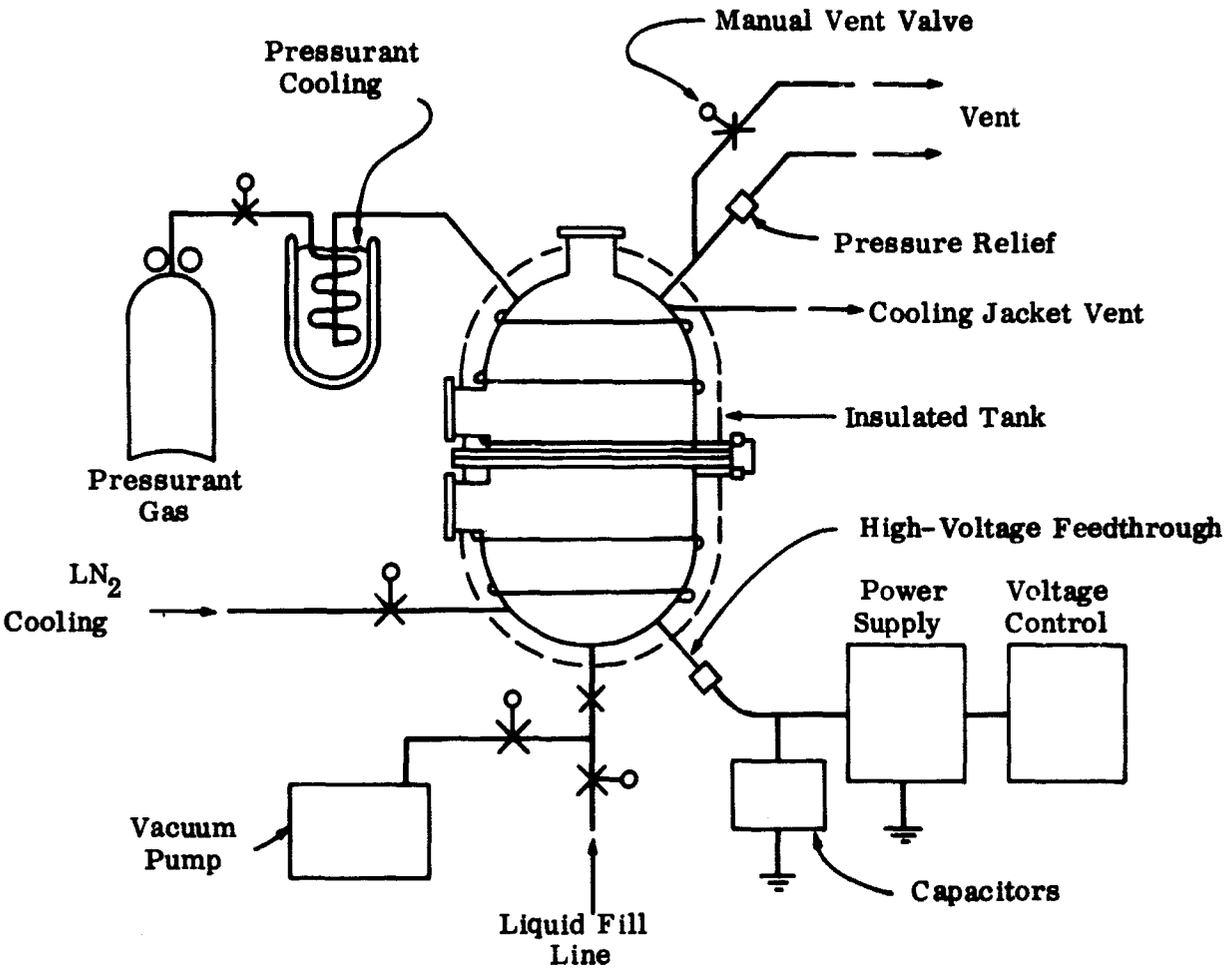

Fig. 2. Cryogenic Pressure Test Apparatus

To test with a gas mixture, step 5 is performed in two parts. For example, to test at 25 per cent helium concentration in oxygen, first pressurize to 10 psig (25 psia) with helium, then to 85 psig (100 psia) with oxygen. The concentration can be changed by pressurizing with one gas or the other, computing the partial pressures of each constituent gas after each pressurization. (This procedure assumes the gas mixture is homogeneous and that any leakage or vented gas is of the same concentration as the bulk.)

To test with LOX, step 5 is also performed in two parts. First, backfill and pressurize to 5 psig with helium. Then transfer LOX under slight pressure, using the manual vent valve to keep the pressure low. The slight tank pressure is to prevent leakage of atmospheric air into the tank where moisture from the air can condense into the cryogen.

Two types of electrodes were used during the tests: 1) polished disc electrodes representing an ideal case, and 2) elemental sections of a typical ribbon electrode mounted on a section of tank wall representative of the actual system geometry (Fig. 3). Breakdown data were obtained for hydrogen and oxygen gas with various concentrations of helium pressurant over the temperature range from 140°R to 535°R, the pressure range from 15 psia to 100 psia, and electrode spacings of 1/2" to 3".

The object of these experiments was to establish parametric breakdown information directly applicable to the engineering design of the ribbon electrode dielectrophoretic liquid expulsion system. The emphasis was not to formulate a fundamental correlation on an analytical basis.

The data have been correlated as a function of the parameter (Pd/T), where P is the absolute pressure, d is the electrode spacing, the T is the absolute temperature. This is the parameter established by the Paschen similitude law for correlating electrical breakdown voltage for geometrically similar electrode configurations.*

*Cobine, J. D., Gaseous Conductors Theory and Engineering Applications, Dover Publications, Inc., New York (1958), § 7.8.

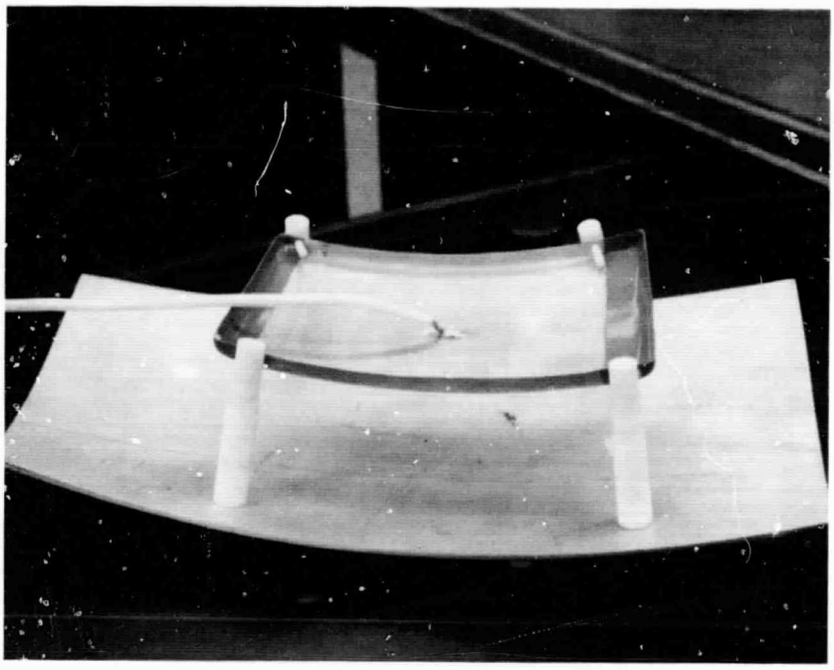

Fig. 3

Electrode Element With Teflon Coating on Ends
to Prevent Premature Electrical Breakdown

3.2 Oxygen/Helium Modular Tests

The oxygen/helium breakdown data* correlates very consistently as a function of the Paschen function (Pd/T) with the helium concentration as a parameter (Fig. 4). Very little corona was in evidence in any of these tests. This is a primary factor in explaining the lack of scatter over the wide range of test conditions considered.

3.3 Hydrogen/Helium Modular Tests

A major phenomenological difference between the oxygen and the hydrogen electrical breakdown is that corona is much more in evidence with the hydrogen. Corona is a non-selfsustaining form of electrical failure. The presence of corona tends to lower the voltage at which spark breakdown occurs by ionizing the gas.

The electrical breakdown of hydrogen/helium mixtures* can be correlated fairly consistently on the Paschen similitude function Pd/T (Fig. 5). Deviations from this correlation can be explained on the basis of two factors.

1. The Paschen function is intended for "geometrically similar" electrode configurations. This is <u>not</u> the situation when a given electrode is used at various spacings.
2. The high corona data points, although plotted in Fig. 5 for completeness, would be expected to give lower breakdown voltages as explained above.

It is important to keep in mind the significance and intended use of this breakdown data. The data is intended only as an aid in making engineering decisions in the design of a dielectrophoretic propellant management system. Such a design must allow for the "worst case" operating situation with a suitable margin of safety. Consequently, the lowest breakdown voltage conditions, pure helium pressurization, set the upper limit on the operating voltage. The value of the other data on pure hydrogen and hydrogen/helium mixtures is merely to: 1) verify that the pure helium case is

---

*The raw breakdown data is tabulated in Appendix A.

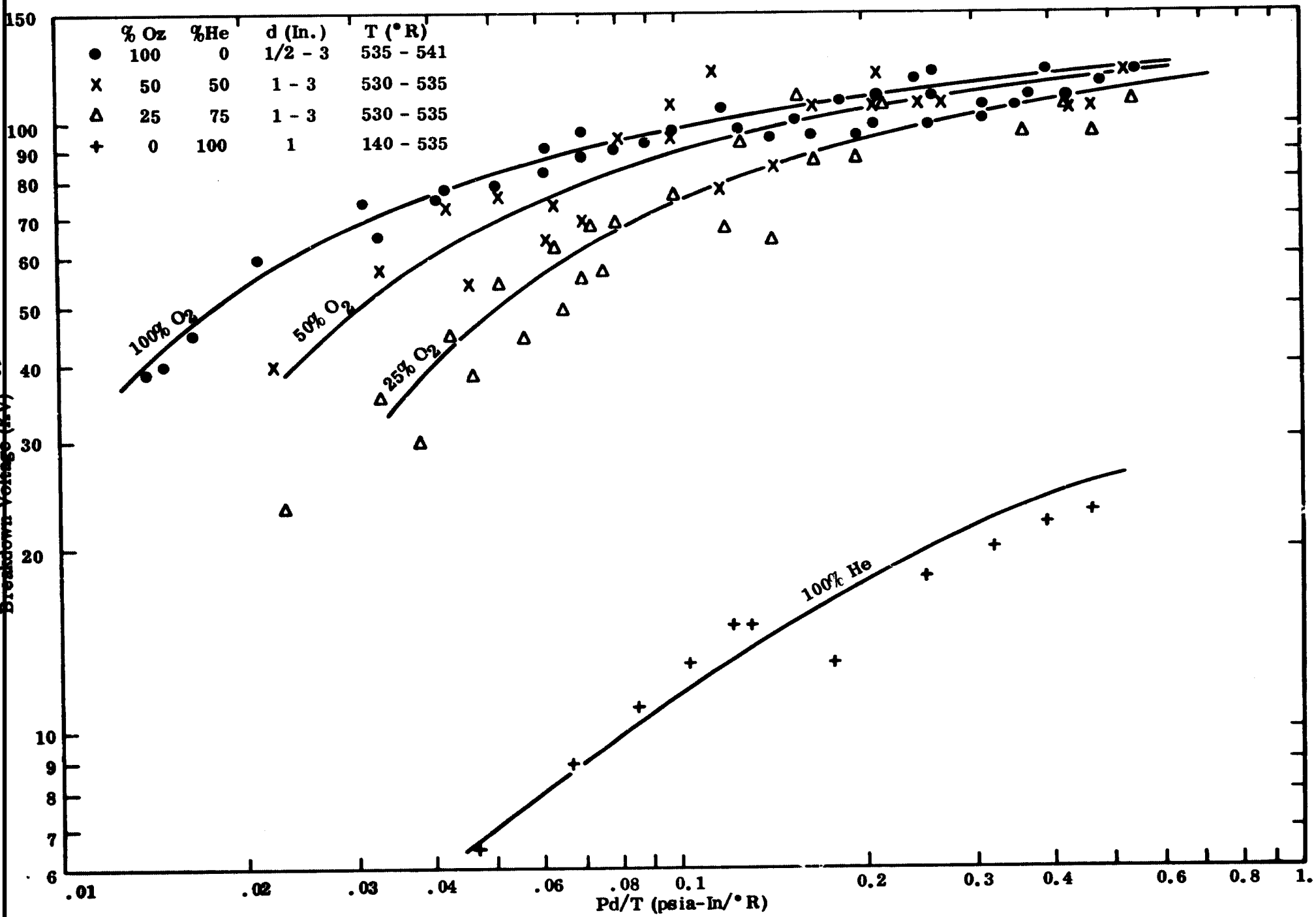

Fig. 4. Breakdown Voltage in Oxygen/Helium Mixtures

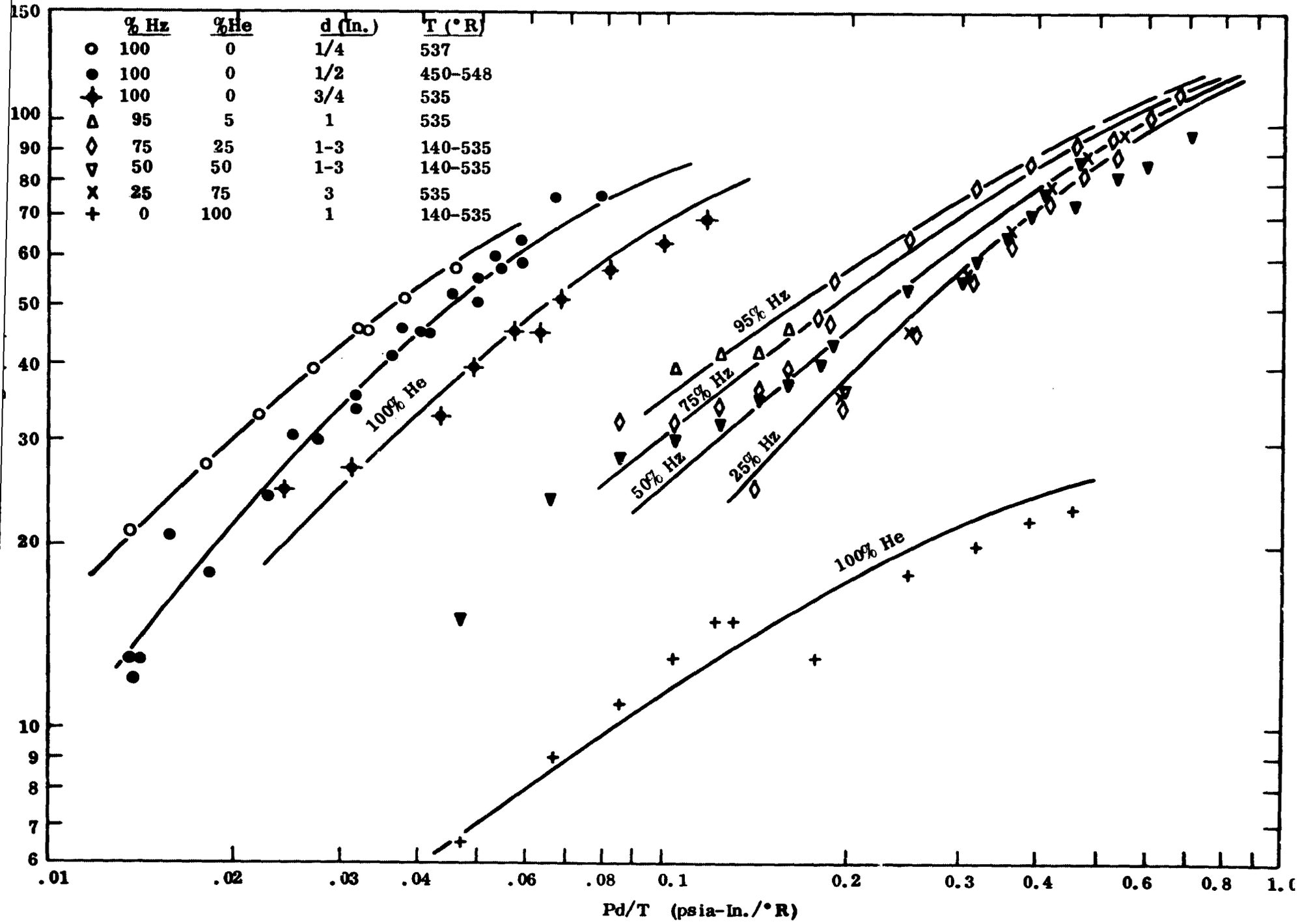

Fig. 5. Breakdown Voltage in Hydrogen/Helium Mixtures

the worst condition for breakdown, and 2) to further demonstrate that electrical breakdown in the hydrogen or hydrogen/helium environment in no way presents a safety hazard.

Section 4
FULL-SCALE TESTS

Full-scale demonstration tests of the ribbon electrode dielectrophoretic propellant expulsion system were conducted for a two-fold purpose.

1. To show that the modular test data on electrical breakdown can be scaled up for the engineering design of full-scale systems.
2. To once again demonstrate the complete safety of the dielectrophoretic system even under the most adverse operating conditions.

4.1 Full-Scale Test Apparatus

The full-scale tests were conducted in a special facility at the Lockheed Missiles and Space Company's Santa Cruz Test Base (Fig. 6). The dielectrophoretic ribbon electrode consisted of 6" wide sections of 0.041" thick formed aluminum channels (Fig. 7) mounted in a 41.5" diameter tank on Teflon supports (Figs. 8 and 9). The two electrode sections were mounted at 1" and 3" spacings from the tank wall. A second set of electrode sections were instrumented with thermocouples and resistance temperature sensors and installed in the same manner as the active electrode (Figs. 10 and 11). The temperature instrumentation was used for measuring both the liquid level in the tank and the thermal stratification in the ullage gas.

The high voltage power was brought into the cryogenic vessel using a special high-voltage feedthrough (Fig. 12). A complete description, analysis, and evaluation of the coaxial feedthrough design is presented in Appendix B.

The 41.5" diameter cryogenic vessel was insulated and installed in a vacuum chamber (Figs. 13 and 14) to minimize heat leakage into the cryogen. The high-voltage feedthrough extended out through the vacuum chamber in a single unit.

4.2 Full-Scale Tests

Breakdown tests in the full-scale apparatus were conducted substantially the same as the small-scale tests.

Fig. 6. Lockheed Missiles and Space Company's Santa Cruz Test Base

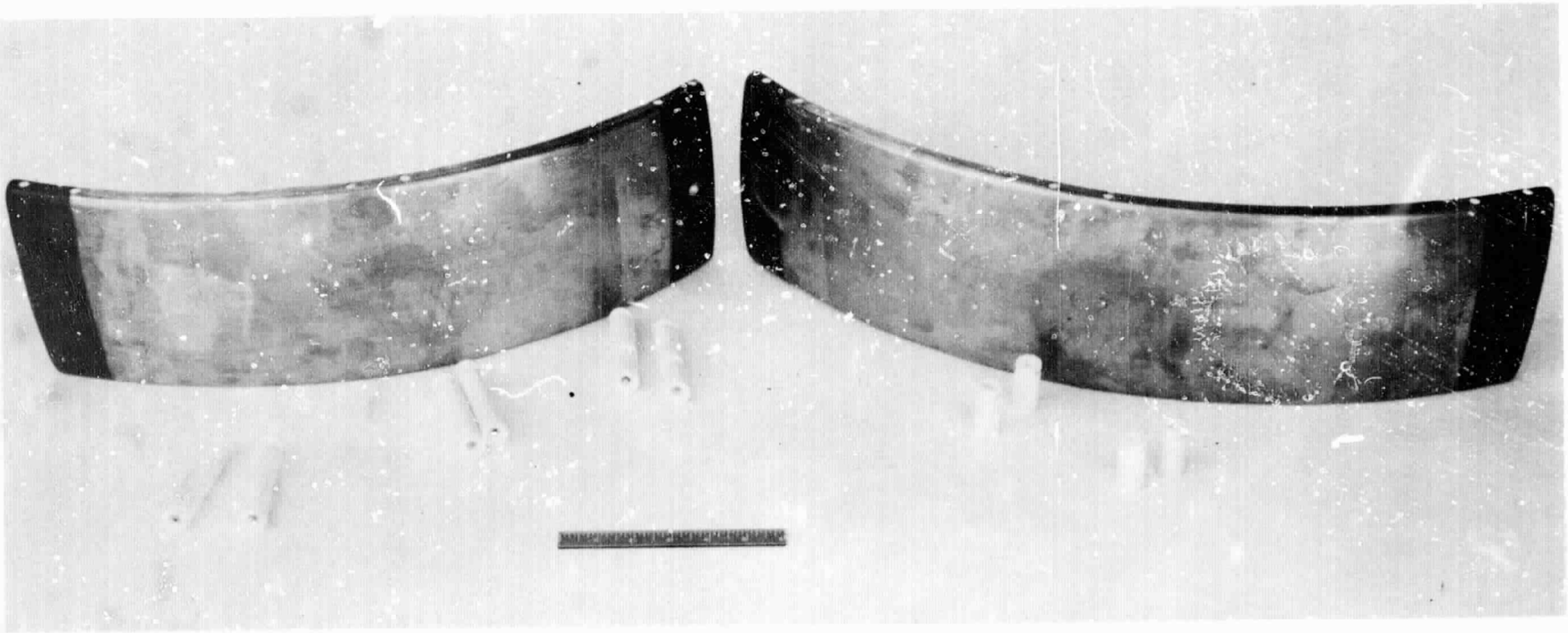

Fig. 7. Ribbon Electrode Sections and Supports

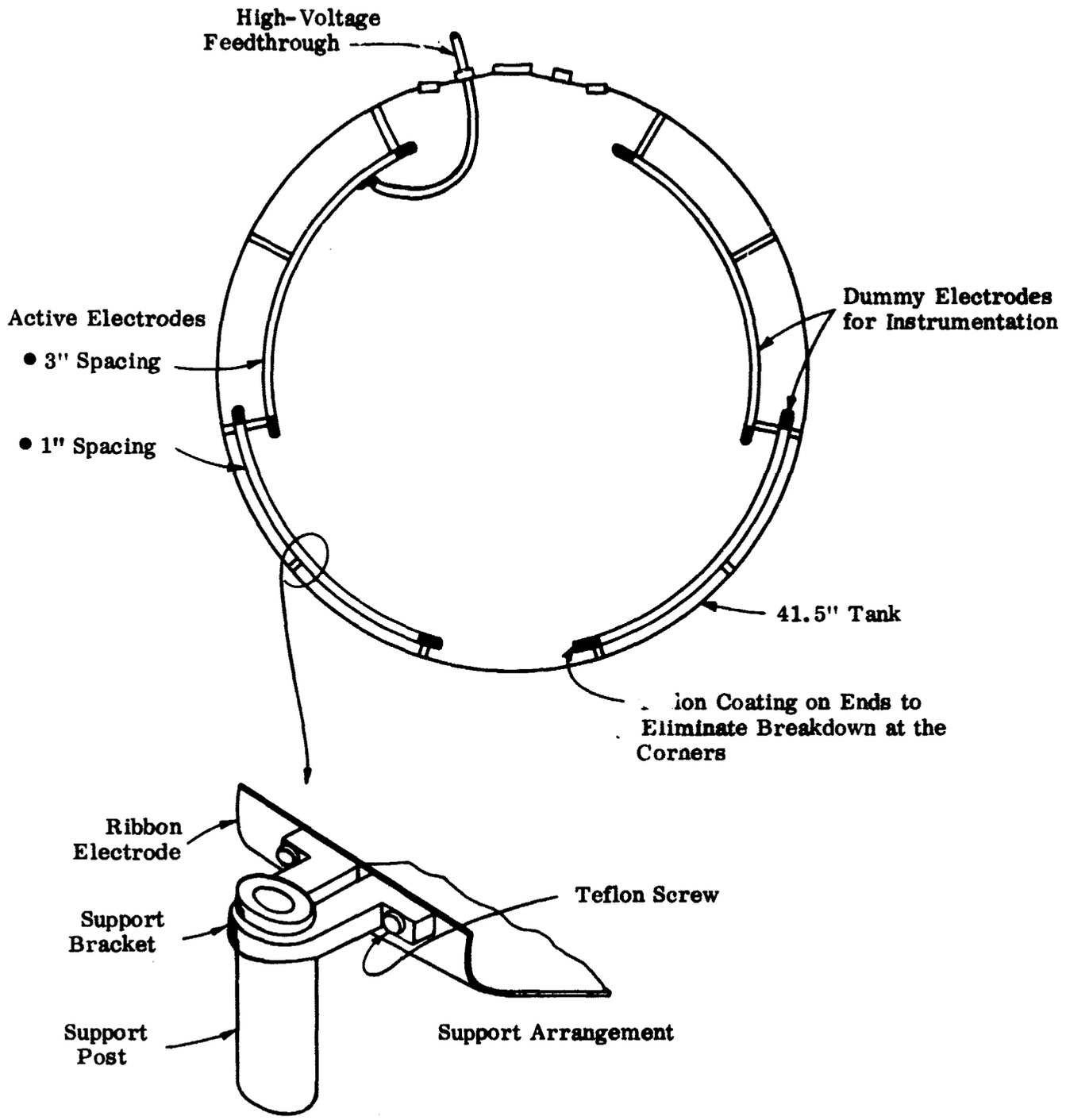

Fig. 8. Electrode and Support Arrangement LMSC Tests

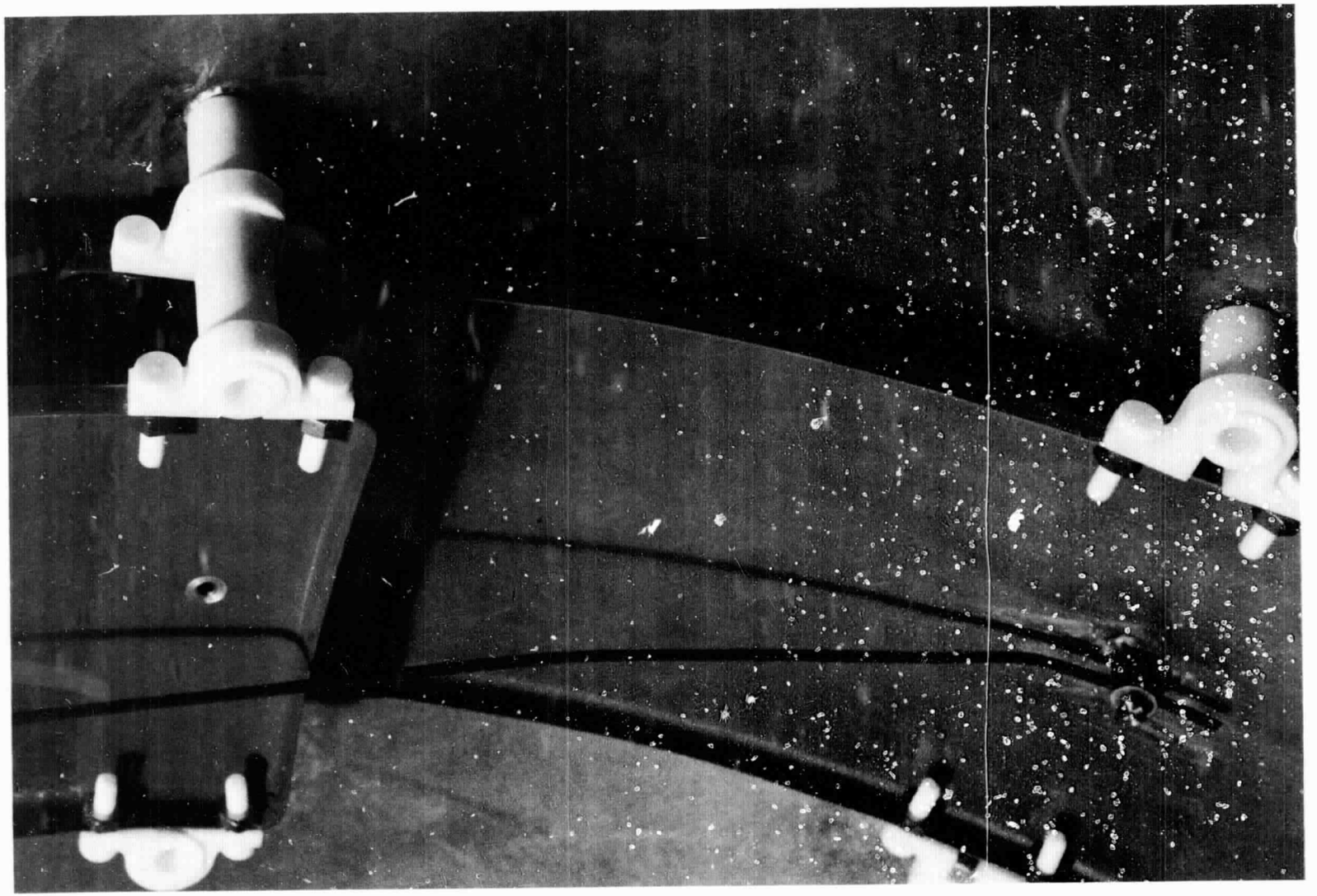

Fig. 9. Electrodes and Supports Assembled in Test Tank

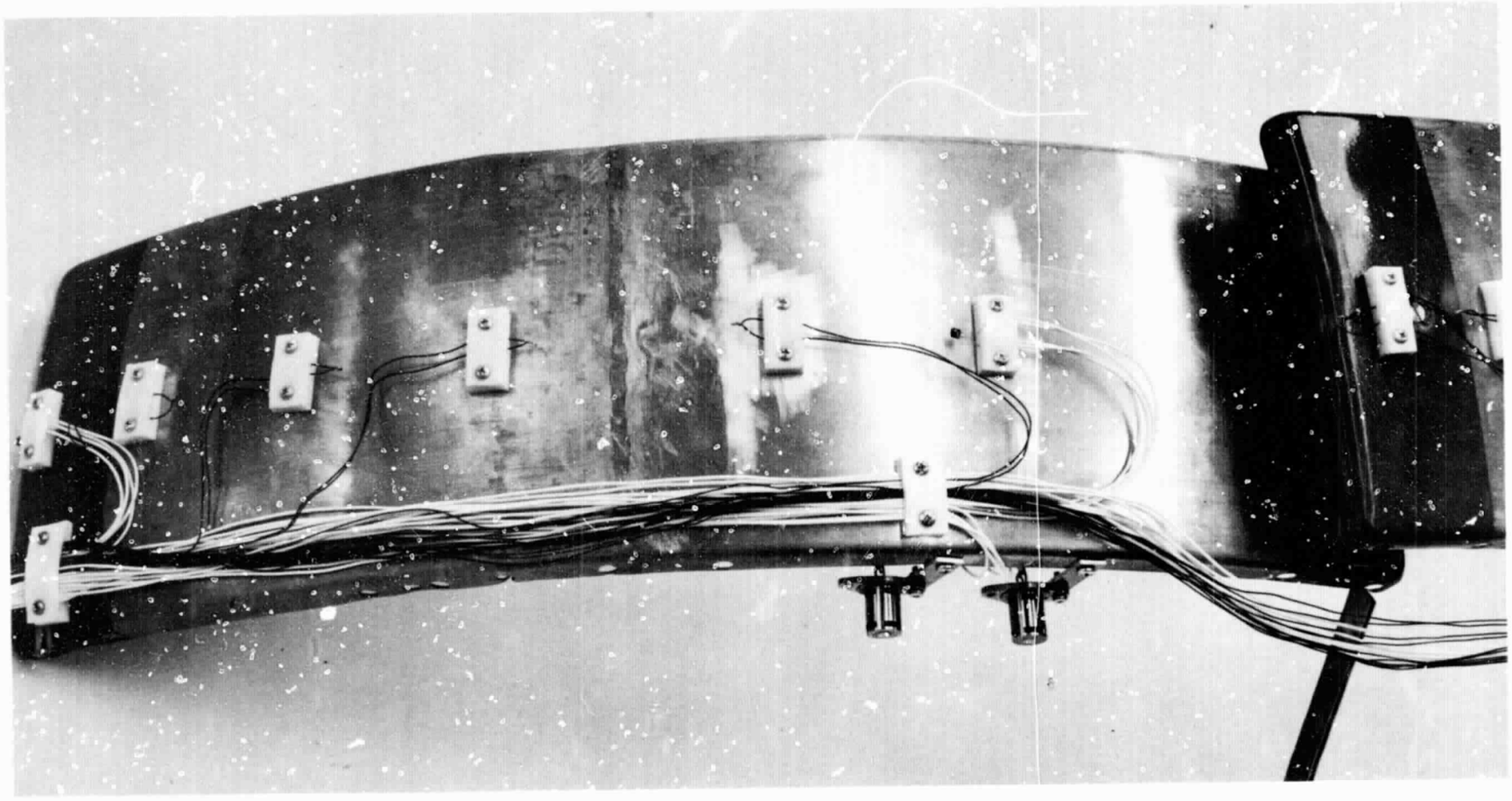

Fig. 10. Instrumentation Electrodes

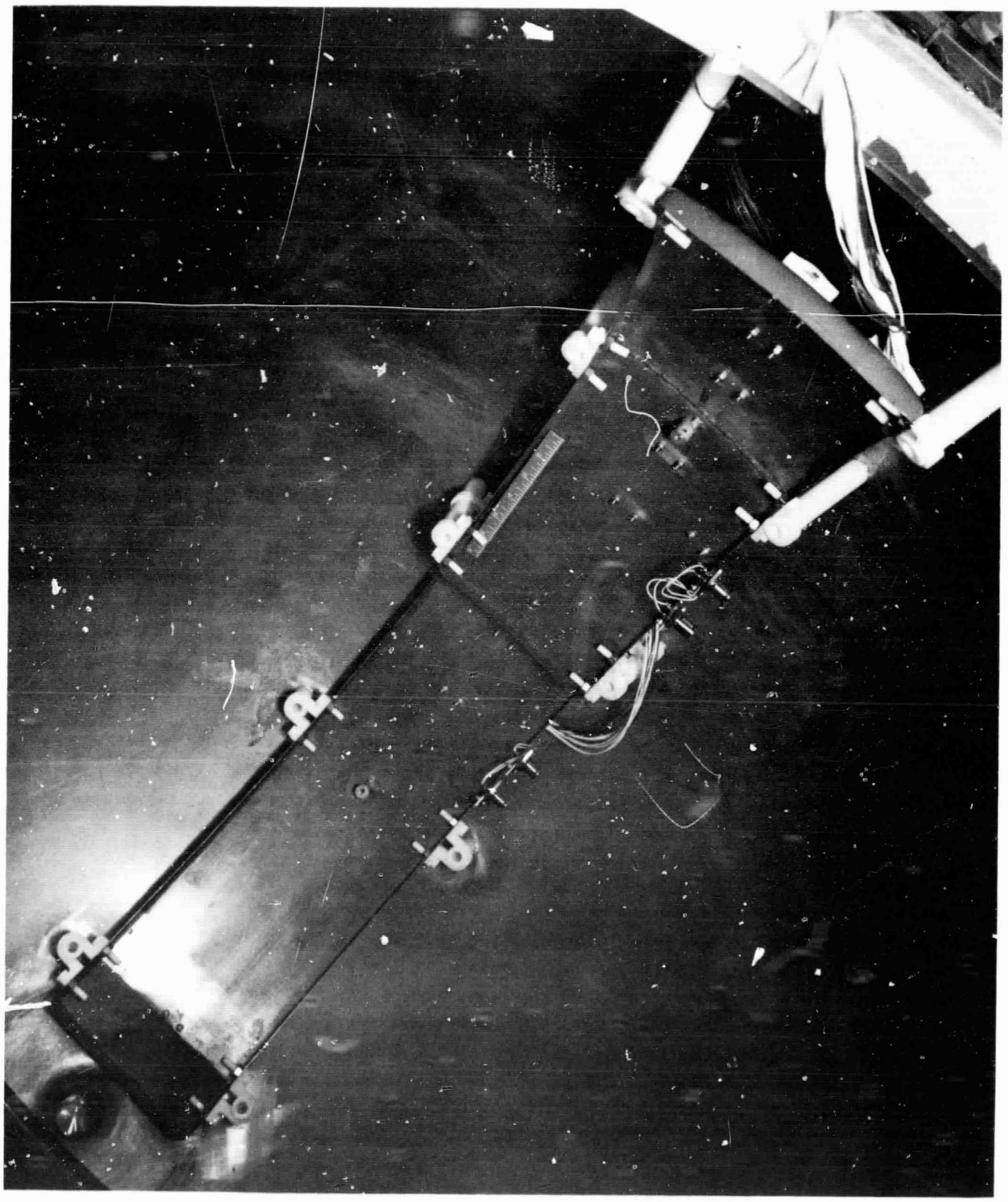

Fig. 11. Instrumentation Assembled in Test Tank

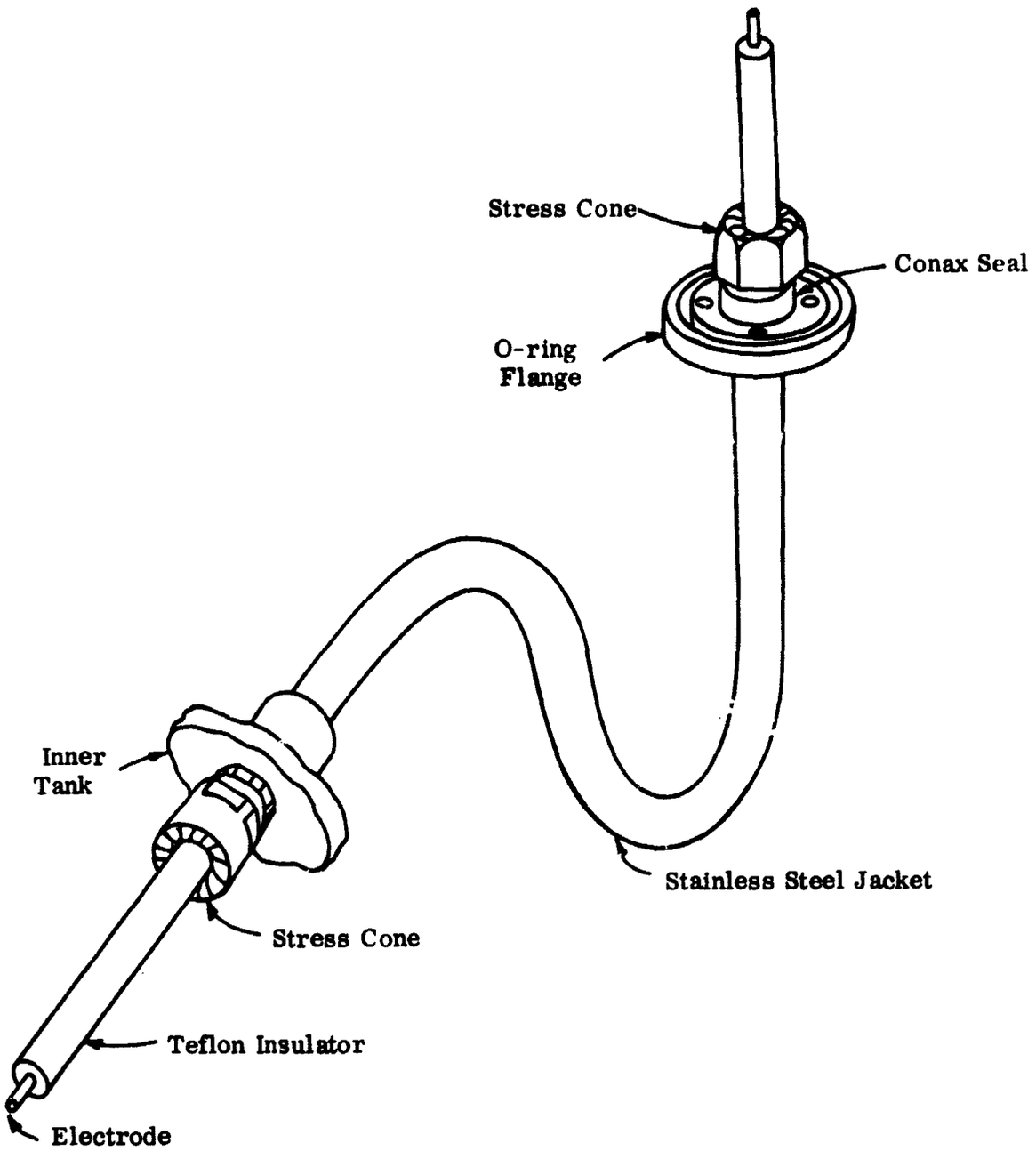

Fig. 12. High-Voltage Feedthrough

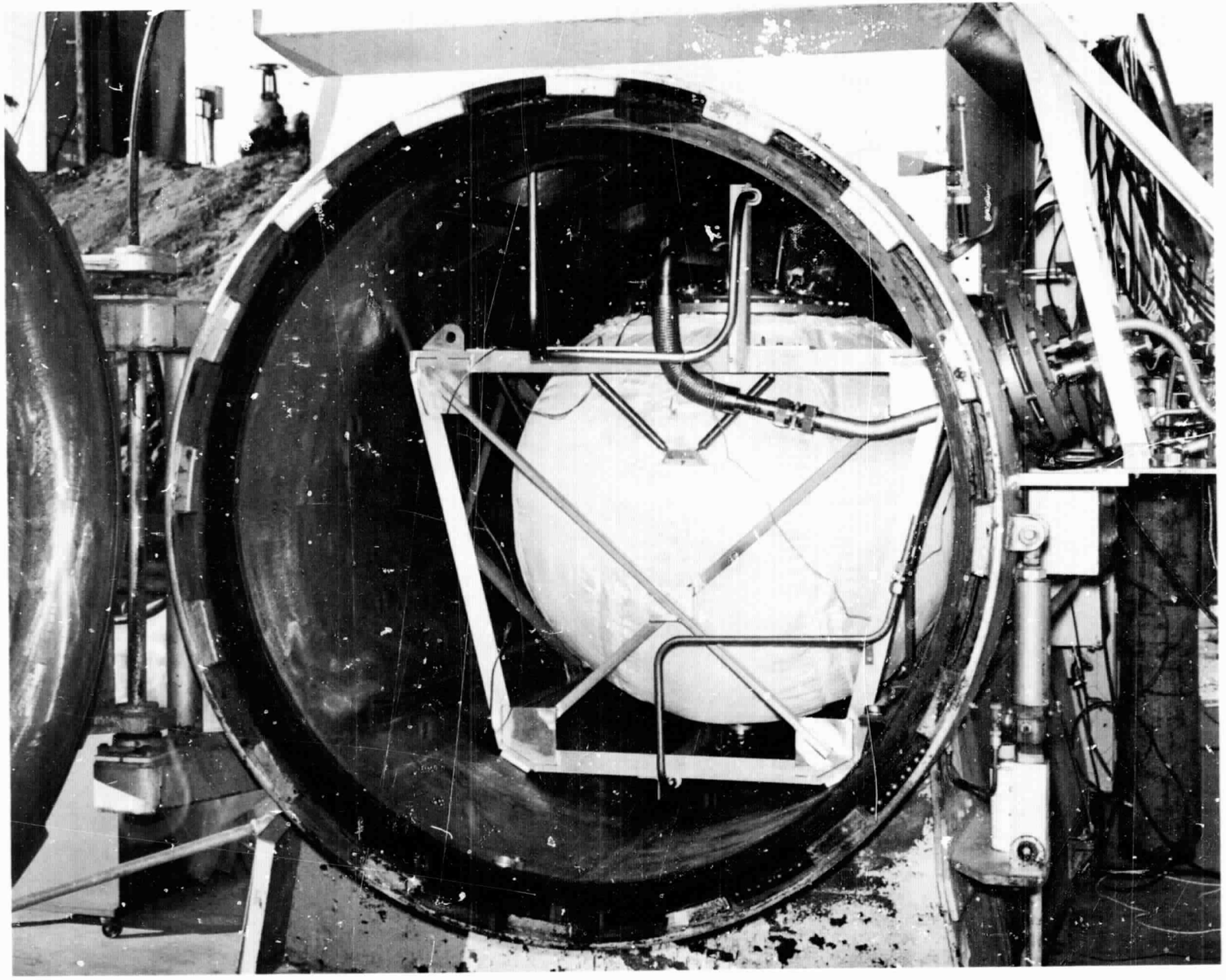

Fig. 13. Cryogenic Test Vessel Installed in Vacuum Chamber

Fig. 14. General Layout of Test Facility

The results of the oxygen and oxygen/helium tests* are shown in Fig. 15 correlated as a function of Pd/T. The modular test results, included for comparison, indicate close agreement for the two sets of tests. The relatively short series of tests with oxygen was caused by the failure of the high-voltage feedthrough.

The results of the hydrogen and hydrogen/helium tests* are shown in Fig. 16. As with the modular tests, corona was substantial in these tests and resulted in a considerable amount of data scatter. If only the low corona data points are considered, the results are in fairly close agreement with the modular test data. In particular, the pure helium data, which is the limiting condition for a dielectrophoretic system design, is in very close agreement.

High energy electrical breakdowns were seen to cause interference with the thermocouple and resistance thermometer readings. The breakdown would cause a surge in the instrument signal. At all other times, other than at the instant of the breakdown, there was no interference of the instrumentation from the dielectrophoretic system.

*Raw breakdown data tabulated in Appendix A.

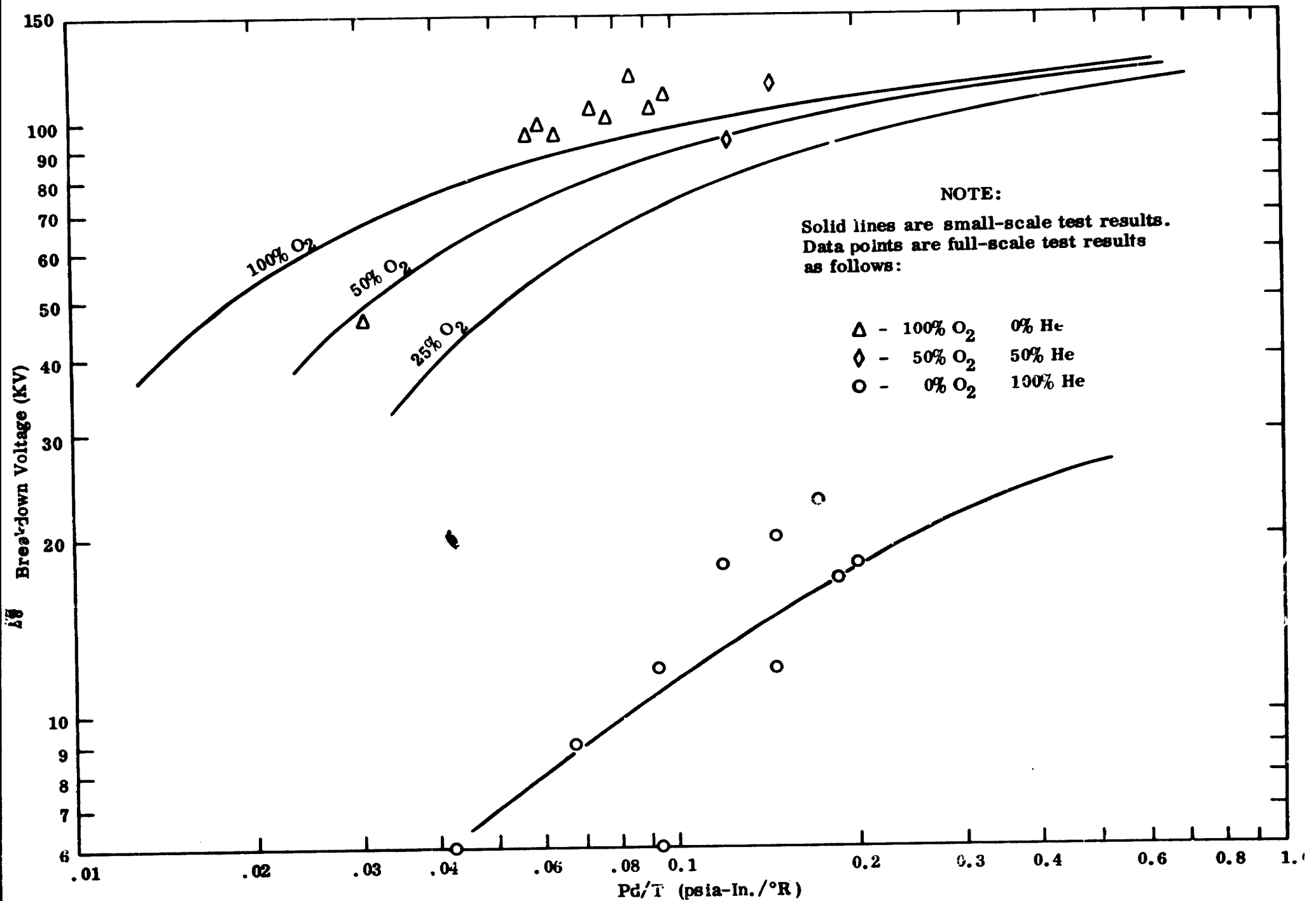

Fig. 15. Full-Sacle Breakdown Tests in Oxygen/Helium Mixtures

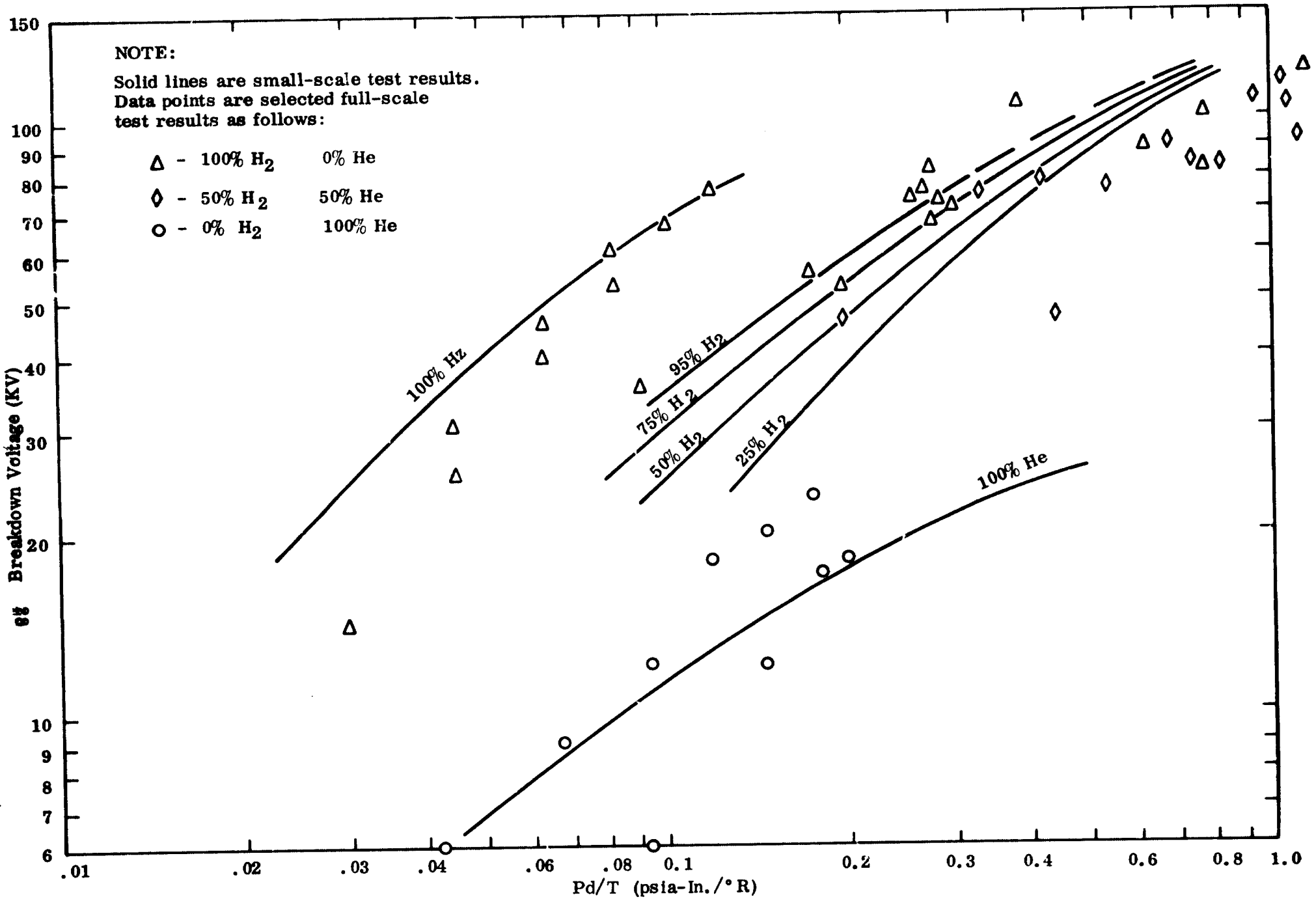

Fig. 16. Full-Scale Breakdown Tests in Hydrogen/Helium Mixtures

Section 5
CONCLUSIONS

1. The dielectrophoretic propellant management system is completely safe with oxygen and hydrogen propellants with helium pressurization over the full range of possible operating conditions.

2. Voltages to 100 KV are practical and electrical breakdown can be avoided by proper attention to geometrical details.

3. Small-scale module electrical breakdown tests can be used to predict the performance of full-scale designs.

4. Special care will be required to further minimize corona in the design of a dielectrophoretic system for use with hydrogen.

5. High energy electrical breakdowns did affect thermocouple and resistance thermometer readings. Under normal operating conditions, the electric field causes no interference with temperature instrumentation.

Appendix A
TABULATED ELECTRICAL BREAKDOWN DATA

Table No.

Table A.1

ELECTRICAL BREAKDOWN DATA
OXYGEN/HELIUM MIXTURES
MODULAR TESTS

Run No.	Data Point	d (In.)	He %	P (psia)	T (°R)	V (KV)	Pd/T
1	1	1/2	0	66	541	90	.061
	2			33		74	.031
	3			23		60	.021
	4			18		45	.017
	5			16		40	.015
	6			15		39	.014
	7			44		75	.041
2	1	3	0	95	535	120	.532
	2			85		115	.472
	3			75		110	.420
	4			65		110	.364
	5			55		100	.308
	6			45		98	.252
	7			35		95	.196
	8			25		94	.140
3	1	1/2	0	95	535	92	.089
	2			85		90	.079
	3			75		88	.070
	4			65		83	.061
	5			55		79	.051
	6			45		77	.042
	7			35		65	.033
	8			25		47	.023

Table A.1 (cont.)

Run No.	Data Point	d (In.)	He %	P (psia)	T (°R)	V (KV)	Pd/T
4	1	1-1/2	0	95	535	120	.266
	2			85		117	.238
	3			75		110	.210
	4			65		108	.182
	5			55		100	.154
	6			45		97	.126
	7			35		96	.098
	8			25		96	.070
5	1	2-1/2	0	85	535	120	.397
	2			75		105	.350
	3			65		105	.304
	4			55		110	.257
	5			45		99	.210
	6			35		95	.164
	7			25		105	.117
6	1	1	50	65	530	120	.116
	2			55		108	.098
	3			45		94	.080
	4			35		73	.063
	5			25		54	.046
7	1	3	50	95	535	120	.532
	2			85		105	.476
	3			75		104	.421
	4			25		83	.140
8	1	1/2	50	65	535	63	.061
	2			55		76	.051
	3			45		73	.042
	4			35		58	.033
	5			25		40	.023

Table A.1 (cont.)

Run No.	Data Point	d (In.)	He %	P (psia)	T (°R)	V (KV)	Pd/T
9	1	1-1/2	50	95	535	108	.266
	2			85		108	.238
	3			75		108	.210
	4			35		95	.098
	5			25		69	.070
10	1	2-1/2	50	45	535	120	.210
	2			35		108	.164
	3			25		77	.117
11	1	1	75	40	530	57	.075
	2			35		49	.066
	3			30		44	.057
	4			25		38	.047
	5			20		30	.038
12	1	3	75	96	535	108	.532
	2			85		95	.476
	3			75		108	.420
	4			65		95	.364
13	1	3	75	35	535	88	.196
	2			25		63	.140
14	1	1/2	75	85	535	68	.079
	2			75		69	.070
	3			65		63	.061
	4			55		54	.051
	5			45		44	.042
	6			35		35	.033
	7			25		23	.023
15	1	1-1/2	75	55	535	110	.154
	2			45		93	.126
	3			35		75	.098
	4			25		55	.070
16	1	2-1/2	75	45	535	107	.210
	2			35		86	.164
	3			25		66	.117

Table A.2

ELECTRICAL BREAKDOWN DATA
HYDROGEN/HELIUM MIXTURES
MODULAR TESTS

Run No.	Data Point	d (In.)	He %	P (psia)	T (°R)	V (KV)	Pd/T	Heavy Corona
1	1	1/4	0	70	537	45	.033	
	2			99		57	.046	
	3			81		51	.038	
	4			69		45	.032	
	5			59		39	.027	
	6			47		33	.022	
	7			38		27	.018	
	8			29		21	.035	
2	1	1/2	0	15	548	13	.014	
	2			25		24	.023	
	3			35		35	.032	
	4			45		45	.041	
	5			55		55	.050	
	6			65		64	.059	
	7			60		57	.055	
	8			50		52	.046	
	9			40		41	.036	
	10			30		30	.027	
	11			20		18	.018	
	12			15		12	.014	
	13			25		24	.023	
	14			35		34	.032	
	15			45		45	.041	
	16			55		50	.050	
	17			65		58	.059	

Table A.2 (cont.)

Run No.	Data Point	d (In.)	He %	P (psia)	T (°R)	V (KV)	Pd/T	Heavy Corona
3	1	1/2	0	67	505	75	.067	
	2			53	503	60	.053	
	3			37	501	45	.037	
	4			24	501	30	.024	
	5			15	501	21	.015	
	6			75	473	75	.079	
4	1	3/4	0	45	535	45	.063	
	2			86		69	.120	
	3			73		63	.103	
	4			59		57	.083	
	5			49		51	.069	
	6			41		45	.058	
	7			35		39	.049	
	8			31		33	.044	
	9			22		27	.031	
	10			17		25	.024	
5	1	1	5	99	535	55	.189	
	2			85		45	.160	
	3			75		41	.142	
	4			65		41	.123	X
	5			55		39	.104	X
6	1	1	25	99	535	47	.187	
	2			85		39	.160	
	3			75		36	.142	
	4			65		34	.123	
	5			55		32	.104	
	6			45		32	.085	X

Table A.2 (cont.)

Run No.	Data Point	d (In.)	He %	P (psia)	T (°R)	V (KV)	Pd/T	Heavy Corona
7	1	1	25	95	140*	112	.680	
	2			85		102	.606	
	3			75		95	.536	
	4			65		92	.465	
	5			55		86	.393	
	6			45		78	.322	
	7			35		65	.250	
	8			25		48	.179	
8	1	3	25	97	535	88	.544	X
	2			85		82	.480	X
	3			75		74	.426	X
	4			65		63	.369	X
	5			55		55	.312	X
	6			45		45	.255	X
	7			35		34	.196	X
	8			25		25	.140	X
9	1	1	50	99	535	43	.187	
	2			95		40	.179	
	3			85		37	.160	
	4			75		35	.142	
	5			65		32	.123	
	6			55		30	.104	
	7			45		28	.085	
	8			35		24	.066	X
	9			25		15	.047	X

*Assumed to be equalized with saturated LN_2 in "infinite" heat exchanger.

Table A.2 (cont.)

Run No.	Data Point	d (In.)	He %	P (psia)	T (°R)	V (KV)	Pd/T	Heavy Corona
10	1	1	50	101	140*	96	.720	
	2			85		87	.607	
	3			75		82	.536	
	4			65		73	.465	
	5			55		70	.393	
	6			45		59	.322	
	7			35		53	.250	
11	1	3	50	85	535	87	.476	X
	2			75		77	.420	X
	3			65		65	.364	X
	4			55		55	.308	X
	5			45		45	.252	X
	6			35		36	.196	X
12	1	3	75	98	535	95	.550	X
	2			85		88	.476	X
	3			75		78	.420	X
	4			65		66	.364	X
	5			55		56	.308	X
	6			45		45	.252	X
	7			35		35	.196	X

*Assumed to be equalized with saturated LN_2 in "infinite" heat exchanger.

Table A.3

ELECTRICAL BREAKDOWN DATA
GASEOUS HELIUM
MODULAR TESTS

Run No.	Data Point	d (In.)	P (psia)	T (°R)	V (KV)	Pd/T
1	1	1	69	535	15	.130
	2		65		15	.123
	3		55		13	.104
	4		45		11	.085
	5		35		9	.066
	6		25		6.5	.047
2	1	1	65	140*	23	.463
	2		55		22	.394
	3		45		20	.322
	4		35		18	.250
	5		25		13	.178

*Assumed to be equalized with saturated LN_2 in "infinite" heat exchanger.

Table A.4

ELECTRICAL BREAKDOWN DATA
FULL-SCALE TESTS

Run No.	Data Point	Fluid	P (psia)	He %	d (In.)	T (°R)	V (KV)	A (ma)	Pd/T
1	1	GOX	15.2	0	1	499	47	1.7	.0305
	2		29.1			506	96	2.8	.0574
	3		49.4			511	111	1.6	.0968
2	1	LOX	14.7			188	102	1.0	.0781
	2		22.7			268	120	0.7	.0847
	3		24.1			266	106	0.7	.0906
	4		19.7			269	105	0.6	.0733
	5		14.7			245	99	0.9	.0600
	6		14.4			227	96	0.9	.0635
3	1		29.8	50		236	94	0.7	.1262
	2		35.3			248	118	1.2	.1423
4	1	GH_2	15.7	0		529	14	4.3	.0297
	2		23.7			533	25	6.0	.0445
	3		33.7			535	39	7.0	.0721
	4		43.7			532	52	7.0	.0821
5	5		53.7			533	66	9.8	.1010
	6		63.7			535	75	9.3	.1190
	7		48.7			533	32	9.5	.0915
	8		43.7			534	60	9.0	.0819
	9		33.7			532	45	7.9	.0634
	10		23.7			531	30	7.5	.0446
6	1	LH_2	14.7			54	75	2.0	.2720
	2		18.7			63	20	9.5	.2970
	3		14.7			55	72	3.2	.2670
	4		18.5			60	70	1.9	.3085
	5		18.7			65	72	8.5	.2875
	6		33.7			88	105	0.9	.3830

Table A.4 (cont.)

Run No.	Data Point	Fluid	P (psia)	He %	d (In.)	T (°R)	V (KV)	A (ma)	Pd/T
7	1	LH_2	14.7	0	1	85	54	1.6	.1730
	2		18.7			69	81	1.5	.2710
	3		21.7			95	37	2.0	.2285
	4		23.7			83	36	1.5	.2855
	5		33.7			96	42	1.2	.3510
8	6		40.7			107	42	1.4	.3805
	7		38.7			103	51	1.8	.3760
	8		37.7			104	33	0.7	.3630
	9		31.7			99	36	1.4	.3205
9	1		29.7		3	115	100	0.8	.7750
	2		23.7			115	87	5.5	.6180
	3		19.7			91	63	2.1	.6500
	4		16.7			90	30	0.9	.5560
	5		17.7			93	27	1.9	.5710
	6		20.2			100	24	0.8	.6060
	7		28.7			110	81	1.5	.7830
	8		23.7			112	60	1.0	.6350
	9		20.7			109	51	2.2	.5690
10	1		38.7			102	120	3.4	1.140
	2		28.7			110			
	3		28.7			63	105	9.1	1.367
	4		28.7			56	84	7.2	1.538
	5		19.7			96	54	5.6	.6160
	6		19.7			84	60	6.9	.7040
11	1		31.7		1	161	51	3.2	.1970
	2		48.7			178	66	3.6	.2740
	3		55.7			178	57	4.1	.3130
	4		43.7			170	36	2.1	.2570
	5		33.7			105	24	2.8	.3210
	6		24.7			109	15	6.3	.2265
	7		18.7			110	9	4.7	.1700

Table A.4 (cont.)

Run No.	Data Point	Fluid	P (psia)	He %	d (In.)	T (°R)	V (KV)	A (ma)	Pd/T
12	1	He	15.3	100	1	365	6	0.7	.0419
	2		25.1			371	9	1.0	.0677
	3		35.1			381	12	0.4	.0922
	4		45.2			379	18	1.6	.1193
13	5		54.7			374	20	1.5	.1462
	6		65.2			378	23	1.2	.1726
	7		75.2			376	18	0.3	.2000
	8		73.7			396	17	0.3	.1862
	9		54.7			375	12	0.3	.1460
	10		33.7			363	6	0.3	.0929
14	1	LH_2	30.2	50		94	75	5.0	.3220
	2		33.7			77	47	9.7	.4380
	3		38.7			73	76	10.0	.5300
	4		43.7			67	90	9.4	.6520
15	5		48.7			131	102	8.3	.3720
	6		63.7			135	120	3.7	.4720
	7		53.7			122	114	6.0	.4400
	8		46.7			111	78	6.7	.4210
	9		14.2			72	45	5.9	.1970
[illegible]	1		30.2		[illegible]	76	90	--	1.190
[illegible]	2		43.7			112	105	0.9	1.170
	3		23.7			97	84	3.0	.7340
	4		33.7			108	108	4.0	.9360
	5		43.7			116	117	0.6	1.130
	6		28.7			104	81	1.9	.8280
17	1		68.7	70		116	120	0.6	1.650
	2		28.7			110	10	1.5	.7820
	3		33.7			101	75	1.0	1.000
	4		48.7			113	90	1.0	1.160
	5		53.7			121	75	0.7	1.332
	6		63.7			122	75	0.6	1.568

Table A.4 (cont.)

Run No.	Data Point	Fluid	P (psia)	He %	d (In.)	T (°R)	V (KV)	A (ma)	Pd/T
18	7	LH_2	15.7	70	3	93	9	0.5	.5070
↓	8	↓	23.7	↓	↓	106	30	6.8	.6700
↓	9	↓	33.7	↓	↓	115	45	1.1	.8800
↓	10	↓	33.7	↓	↓	112	60	0.7	.9030
↓	11	↓	41.7	↓	↓	120	75	0.7	1.042
19	1	↓	63.7	↓	1	114	117	0.7	.5580
↓	2	↓	23.7	↓	↓	94	108	0.7	.2520
↓	3	↓	23.7	↓	↓	113	117	0.8	.2095

Appendix B
HIGH-VOLTAGE FEEDTHROUGH DESIGN

A new low heat-leak, high-voltage feedthrough concept was developed for penetrating superinsulated propellant tanks. The design consists of a Teflon insulated, high-voltage lead passing through a thin walled stainless steel tube. This tubular jacket is welded to the propellant tank on one end and to a gland-type pressure seal on the other. The length of the feedthrough is brought through the multi-layer tank insulation in a spiral to minimize radiational heat leaks. The length of the feedthrough is determined to minimize the conductive heat leak. The gland seal is maintained at ambient temperature and provides a very effective pressure sealing of the feedthrough assembly.

To analyze the heat leakage of the coaxial feedthrough design, the feedthrough can be modeled as in Fig. B.1.

The total heat leak through the feedthrough is given by

$$Q = \left(\frac{A_S}{L}\int_{T_C}^{T_H} \lambda\, dT\right)_{\text{Steel}} + \left(\frac{A_T}{L}\int_{T_C}^{T_H} \lambda\, dT\right)_{\text{Teflon}} \qquad \text{(B.1)}$$

where

- Q = heat leak
- A = cross-sectional area
- L = length
- λ = thermal conductivity
- T_C = cold-end temperature
- T_H = warm-end temperature

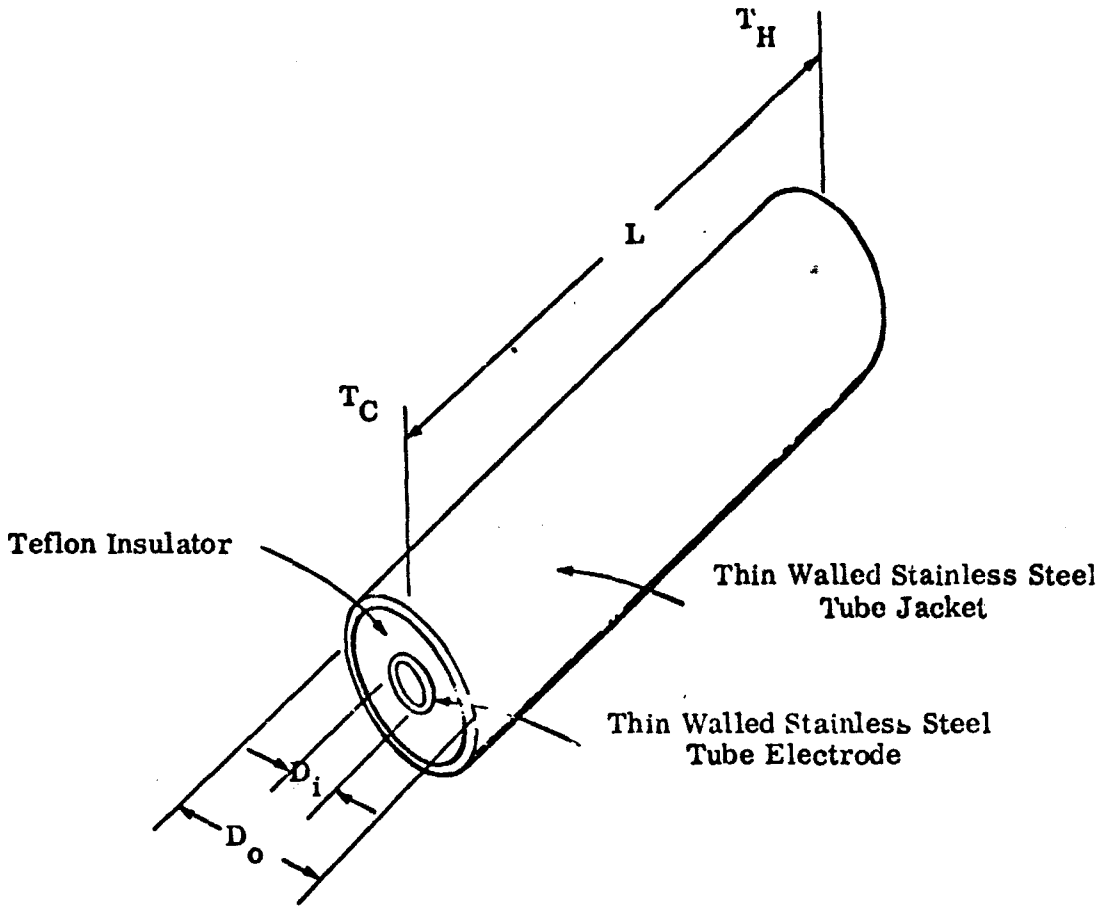

Fig. B.1. Model for Heat Leak Analysis of the Coaxial High-Voltage Feedthrough

From the literature* the conductivity integral over the range from saturated liquid oxygen and hydrogen temperature to ambient temperature for stainless steel and Teflon is:

	$\int_{T_C}^{T_H} \lambda \, dT \quad \left(\frac{\text{Watts}}{\text{cm } ^\circ\text{K}}\right)$	
Material	LH_2 (20° - 300° K)	LO_2 (90° - 300° K)
Stainless	30.437	26.24
Teflon	0.6856	0.539

Substituting the appropriate relationships for the areas and the conductivity integrals, Eq. (B.1) reduces to:

$$Q = \frac{(D_o + D_i)}{L}\left[\, 210t + 1.08\,(D_o - D_i)\,\right] \text{ for oxygen}$$
$$Q = \frac{(D_o + D_i)}{L}\left[\, 243t + 1.37\,(D_o - D_i)\,\right] \text{ for hydrogen} \qquad \text{(B.2)}$$

where the dimensions are in inches.

An analysis of the weight of the coaxial high-voltage feedthrough was conducted. The weights are presented as a function of the operating voltage and the design heat leak rate in Fig. B.2.

It should be noted that ever at a design heat leak of 0.05 watt (less than 10 per cent of the total heat leak in a superinsulated 40" hydrogen tank) the feedthrough is only a small fraction of the total weight of the dielectrophoretic liquid expulsion system.

*Stewart, R. B., and Johnson, V. J., "A Compendium of the Properties of Materials at Low Temperatures (Phase II), "WADD-TR-60-56 Part IV (December, 1961).

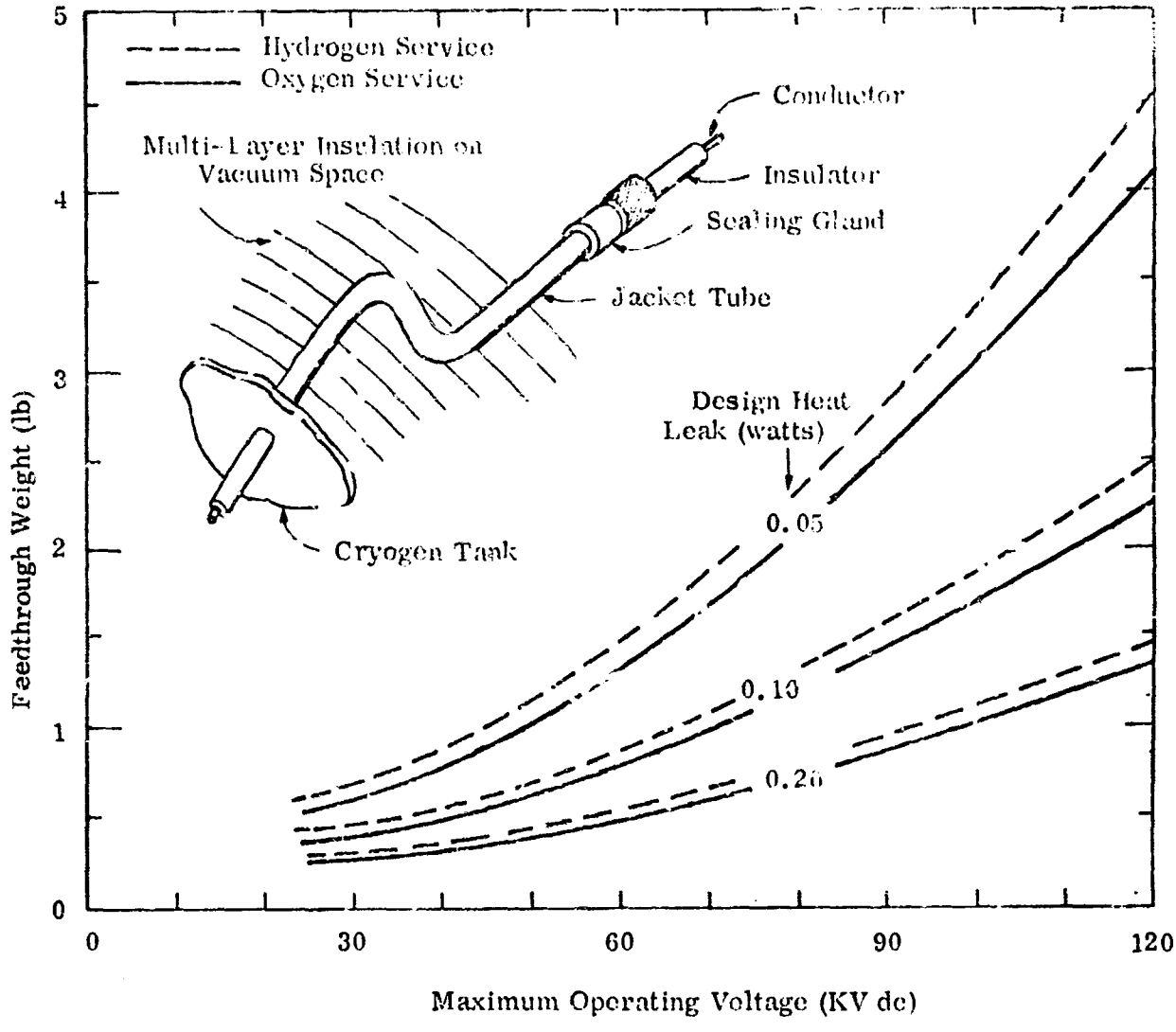

Figure B.2. Weights of Coaxial High-Voltage Feedthrough for Dielectrophoretic Liquid Expulsion Devices for Cryogenic Tankage

Preliminary electrical tests of two coaxial feedthrough geometries have been conducted. Both test models used a 1/4" diameter center electrode. One unit had 1/8" thickness of Teflon insulation while the second model had 1/4" insulation thickness. The first unit performed satisfactorily at up to 60 KV with a factor of safety, while the second unit was operated at 120 KV (the maximum voltage limit of the laboratory power supply).

In the full-scale ribbon electrode tests conducted at the Lockheed Santa Cruz Test Base (see Section 4), two feedthroughs of the 120 KV design were tested. Both of these feedthroughs failed, one in liquid oxygen at 118 KV and one in liquid hydrogen at 117 KV.

This section of the Appendix is incomplete pending examination of the damaged feedthroughs when they are returned from Lockheed.